High-resolution time resolved spectroscopy of collisionless molecular beams. II. Energy randomization and optical phase relaxation of molecules in crossed laser and molecular beams

K. E. Jones, A. Nichols, and A. H. Zewail

Arthur Amos Noyes Laboratory of Chemical Physics, [a] *California Institute of Technology, Pasadena, California 91125*

(Received 17 October 1977)

This paper outlines new ways for separating the different channels of optical dephasing of molecules in beams. It is shown that both the population loss and the optical phase relaxation rates can be obtained under *collisionless conditions* (molecular beams). These dephasing rates, which measure directly the homogeneous width of the prepared resonance, can be obtained with an energy resolution of better than one part in 10^8. Under these conditions the solution of the density matrix equations of motion is given for effusive and nozzle beams which represent a *statistically open ensemble*. The results, which we applied to our recent measurements of optical T_1 and T_2, are discussed in different limits of power broadening, beam geometry, detector characteristics, temperature of the oven (or material container), and the transit time the molecules of different velocities spend in the laser beam. Furthermore, we indicate that the treatment of coherent transients in beams utilizing conventional Bloch equations is not valid since there is a loss of optically excited molecules. Finally, we discuss possible differences between small and large molecules when they undergo radiationless (or reactive) processes following the selective laser excitation (~ 10 kHz–10 MHz).

I. INTRODUCTION

Questions about the nature of energy and phase randomization in molecules are increasing in number. The emphasis is on in what manner and how quickly the excitation energy is distributed "microscopically" within the molecule. This phase and energy randomization problem is of direct relevance to the recent discovery of laser selective chemistry and laser induced multiphoton dissociation of molecules. The current theory for describing these photochemical processes is connected to the theory of radiationless transitions[1–4] in molecules that are nonreactive when excited with light. Although many beautiful experiments have already been conducted in photochemically reactive systems, there remains, however, the question of how *intra* and *inter*molecular relaxation processes take place.

Laser-induced fluorescence has proven useful in mapping out the population distribution in the different states of the system. Further, the method teaches us more about the role of microscopic state-to-state rate constants in determining the overall probability of the energy randomization process.[5] These optical T_1 studies find whether or not intramolecular (vibrational–rotational) relaxation is rapid enough to cause complete thermal equilibrium on the time scale of the experiment. If such a situation is achieved, as in thermal collisional excitation and almost all cases of chemical activation, the well-known RRKM theory can be used since the statistical limit is recovered. In this limit, even if the excitation process is a selective one, the density matrix of the "two levels" (involved in the excitation) is diagonal. In other words, the phase relaxation time (T_2) is essentially zero. If, however, optical T_2 is nonzero (i.e., the off-diagonal elements of the density matrix are not completely averaged out) then we must consider both the energy relaxation mechanisms as well as the homogeneous fluctuations due to phase interruptions in the whole ensemble. Optical dephasing rates (see Fig. 1) cannot usually be obtained by conventional optical techniques. Recently, we have presented a laser emission technique[6–9] for measuring optical T_1 and T_2 in bulbs and in beams with a resolution of better than one part in 10^8.

Molecular beam[5,10–16] experiments are very valuable for many reasons. Firstly, because collisions are absent, one should be able to study intramolecular processes. With the high energy resolution of the laser, the energy can be "deposited" selectively into a small region of the molecule and the evolution from a quasi-stationary or nonstationary (e.g., superpositions of normal modes) state can be examined through the measurement of T_2. We believe that different modes of excitation, together with the measurements of dephasing rates, are extremely important for the understanding of state-to-state photophysical or photochemical dynamics. Secondly, beams can be designed in a way to reduce Doppler broadening. Finally, they provide possibilities for studying space and time resolution along the beam.

However, there are two problems encountered when doing experiments in beams. First, there is the question of can we detect coherent transients (which give the dephasing rates) in a low-density beam. Second, in beams the system is statistically open, i.e., there is no collisional relaxation to keep the overall two-level population constant, and hence conventional (optical) Bloch equations[17] cannot be used. Furthermore, as the molecules traverse the laser beam with different velocities, the coherent interaction between the

[a] Contribution No. 5677.

 0021-9606/78/6907-3350$01.00

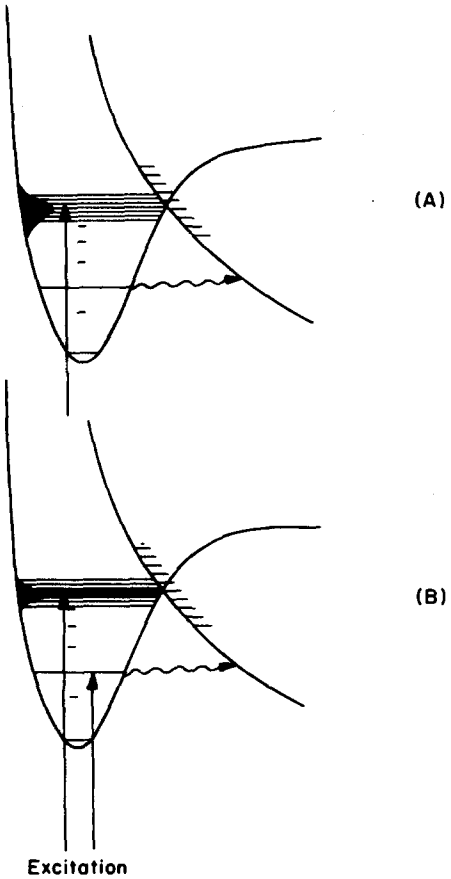

FIG. 1. Potential energy surfaces of bound states interacting with a dissociative manifold. The low energy excitation may give products by tunneling effects. The important point to note in the high energy excitation is that even though the population area (black resonances) may be the same in A and B, the top surface shows a much larger dephasing rate than the bottom one. This means that if the reactive scattering occurs, A will sample more states of the product. The intensity of black resonances do not have any meaning in relation to the reaction coordinate; they just indicate the characteristic of the resonance in the usual intensity vs energy plots.

radiation field and the molecules will be different. For example, slower molecules will be driven to population saturation at a much shorter distance from the illuminated boundary than faster molecules. At any point in space along the illuminated section there will be different molecules which have interacted with the laser field for different periods of time.

In a series of papers we will focus on the above-mentioned problems and examine the nature of energy and phase randomization in reactive and nonreactive molecular processes at *zero pressure*. In an early note[8] (henceforth referred to as I) we have shown that both optical T_1 and T_2 can be measured in a collisionless beam. This paper (1) outlines the nature of coherent optical effects in nozzle and effusive beams; (2) examines optical T_1 and T_2 processes and finds their connection to energy and phase randomization in beams; (3) gives explicit solutions of the density matrix for the transients of collisionless open systems, a point that was not considered before[18]; (4) describes the effects of beam geometry and detector characteristics on the observation of the transients; and finally (5) compares the theory with our recent experimental findings. Also, comparison with the theory that is applicable to bulbs will be made using the density matrix formalism.

II. OPTICAL DEPHASING IN MOLECULAR BEAMS

The problem treated here is that of a laser beam interacting *coherently* with a molecular beam. The molecules in the beam represent a two-level ensemble that is statistically open. The two- levels $|a\rangle$ (excited) and $|b\rangle$ (ground) are assumed (see Fig. 2) to be selected by a radiation field (frequency ω) of the form

$$E(z,t)=\tfrac{1}{2}\mathcal{E}(z,t)\exp[-i(\omega t-kz)]+\text{c.c.} \tag{1}$$

The amplitude of the field $\mathcal{E}$ can vary spatially along the propagation direction z and/or temporally.

The interaction between the molecular ensemble and the radiation field of Eq. (1) give rise to the following total (semiclassical) Hamiltonian:

$$\mathcal{H}=\mathcal{H}_0+\mathcal{H}_{\text{int}}$$
$$=\begin{pmatrix}\frac{\hbar\omega_0}{2} & 0\\ 0 & \frac{-\hbar\omega_0}{2}\end{pmatrix}+\begin{pmatrix}0 & -\mu\cdot\mathbf{E}(z,t)\\ \text{c.c.} & 0\end{pmatrix}, \tag{2}$$

where ω_0 is the transition frequency and μ the transition dipole matrix element.

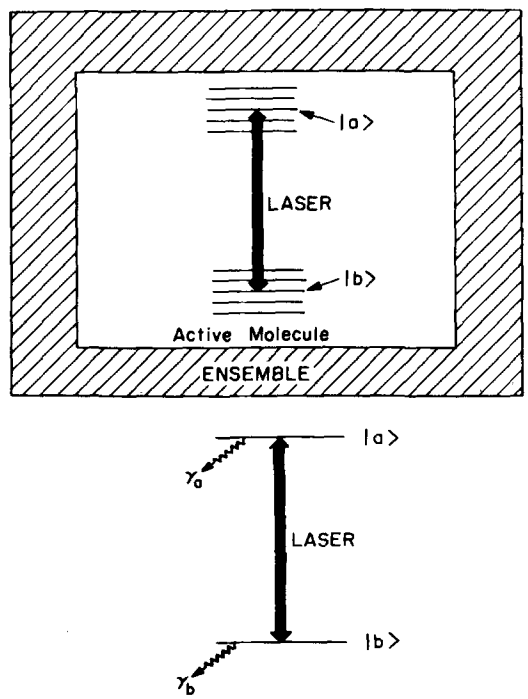

FIG. 2. The laser selection of two-level molecules out of the many levels of the ensemble. The top drawing shows the partition of the whole ensemble into an "optically active" molecule and a large reservoir of optically inactive molecules. The bottom drawing is the equivalent of the top one when theory of optical relaxations is considered (see text).

For a statistically closed system,[17,19] the equation of motion for the density matrix[20] describing the ensemble can be written as

$$i\hbar\dot{\rho}'(t) = [\mathcal{H}, \rho'(t)] + (\text{relaxation terms}), \tag{3}$$

and as shown by the well-known Feynman–Vernon–Hellworth (FVH) description,[21] the system can be described by the following three-component R vector:

$$R_1 = \rho'_{ab} + \rho'_{ba}, \tag{4a}$$

$$R_2 = i(\rho'_{ab} - \rho'_{ba}), \tag{4b}$$

$$R_3 = \rho'_{aa} - \rho'_{bb}. \tag{4c}$$

Similar to NMR,[22] this vector R precesses about an effective field that is determined by the magnitude of the interaction $\mu \cdot \mathbf{E}$, and the transition frequency ω_0. The component R_3 is termed the population difference between the ground and the excited states, and R_1 and R_2, which are given by the off-diagonal elements of the density matrix, are referred to as the *in-phase* and *out-of-phase* components of the polarization that is induced by the laser. In terms of the rotating frame[23] coordinates (e.g., $\rho_{ba} = e^{-i\omega t}\rho'_{ba}$), the macroscopic polarization which is given by[24,25]

$$P = \mu[\rho_{ab}e^{-i\omega t} + \rho_{ba}e^{i\omega t}]$$
$$= \mu[r_1 \cos\omega t - r_2 \sin\omega t] \tag{5}$$

acts as a source term in Maxwell's equations to yield (under the usual assumption of slowly varying envelopes[24] for the electric field and polarization amplitudes; $\mathcal{E}$, $\mathcal{P}$, respectively) the following coherent field[25]:

$$\mathcal{E}_c \simeq -i\frac{\omega L\eta}{2c\epsilon}\mathcal{P}. \tag{6}$$

This field can be "picked up" on the top of the initial laser field. The molecular density is included in $\mathcal{P}$. In the above expressions, L is the sample length, ϵ the background dielectric constant of the medium with η the corresponding refractive index, c the speed of light, and r_1 and r_2 are the rotating frame values of R_1 and R_2, respectively. The important point about Eq. (4) for *statistically closed systems* is that the ensemble coherence is sufficiently described by R_1, R_2, and R_3 and that R_4 is *one* at all times. For *statistically open systems* like those of molecules in a collisionless beam, one must consider R_1, R_2, R_3, *and* R_4 since the total population ($R_4 = \rho_{aa} + \rho_{bb}$) is also changing in time. This point was not considered before.[18]

A collisionless molecular beam has the ability to isolate purely intramolecular processes from molecule–medium interactions as has been mentioned previously. Thus, a precise measurement of parameters characterizing intramolecular dynamics by techniques as the free induction decay (FID) is facilitated by the use of such a collisionless environment.

The peculiar physical and geometric circumstances under which molecular beam spectroscopy is conducted justifies the inquiry as to the applicability of traditional[25,26] theoretical FID expressions to this domain. In the following we provide an exact solution for the density matrix equations which describe molecules in crossed laser and molecular beams.

A schematic of the molecular beam geometry is shown in Fig. 3. The molecules contained in the reservoir or oven (depending upon the vapor pressure of the substance of interest) exit through some suitable aperture, drawn in the figure as a slit parallel to the z axis and normal to the y axis. Equipped with a slit the beam would be a subsonic effusive source of molecules, though the present analysis is generally applicable to supersonic nozzle sources. Detailed descriptions of such sources will not be provided.[27] The single mode laser beam is oriented in front of the slit parallel to the z axis.

At this point we note the molecular beam is not collimated in order to reduce the Doppler spread of the inhomogeneous line. As shown by the FID experiments of Zewail *et al.* performed on I_2, the transition linewidth ($1/\pi T_2$) is very narrow (128 kHz) in the beam (see Paper I). This means that practical considerations concerning laser stability and molecular density dictate that collimation would be futile unless extraordinary measures were taken. The lack of collimation in the molecular beam allows us to ignore the more subtle question of the effect of a noncollimated laser beam,[28] provided the light beam width is reasonably uniform in the interaction region.

Since there is not collimation of molecules (i.e., single slit), the resonance will be inhomogeneously broadened. Thus power broadening effects will be present which tend to damp the FID transient more quickly as power is increased, a result which appears in present FID theories.[26] Since the power broadening damping effect is uninteresting and tends to destroy the FID signal, these experiments are generally performed with the minimum possible laser power. Furthermore, past work has shown that optimum conditions for observing coherent transients occur for minimum possible detector sizes relative to the transverse laser beam profile.[29] Thus we assume that a tightly focused laser beam is not employed and that the detector size is somewhat smaller than the laser profile. This motivates our initial approximation that the molecules of interest will "see" a laser beam with a flat edge as they

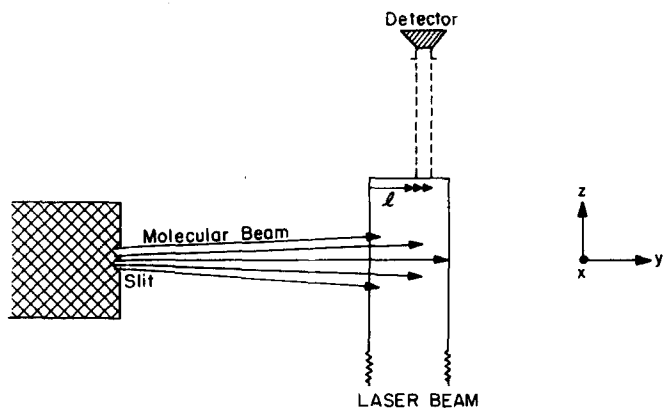

FIG. 3. Laser excitation of beam molecules of different velocities. This geometry is what we used in treating transients by the density matrix approach. The position of detector relative to the laser edge is denoted by l.

enter it (Fig. 3), i.e., at some time t when observing the FID signal only those molecules positioned in front of the detector will contribute and all of these molecules will have entered the laser beam at essentially the same place. It is worth mentioning that the resultant FID signal is not expected to exhibit a strong dependence on the shape of the detector provided it is suitably small. We assume flat edges for convenience.

The transverse Gaussian profile (TEM_{00}) of the laser will be replaced with a square-block-type function, thus providing us the luxury of a soluble model. This shortcoming is not as serious as it first appears for the following reason. The aforementioned small optimum detector size is a result of an effort to try to select a homogeneous or constant intensity section of the laser profile. This suggests that in practice the laser beam should be spatially filtered to allow for a more homogeneous profile similar to the one we select. It should be mentioned that the FID decay expressions by which experimentalists fit their data for gas or solid phase work do not include these Gaussian profile effects.

Conventionally a FID experiment is performed in the following fashion. A laser at some well-defined frequency ω is applied to the sample for some time long enough ($\gg T_1$ the longitudinal relaxation time) such that the system has reached a steady state and a coherent macroscopic polarization [Eq. (5)] exists in the medium. If the laser frequency is now suddenly switched at some time τ, the macroscopic polarization will decay freely provided the new laser frequency is sufficiently removed from the original one, the net effect being that the laser is effectively shut off. After time τ the laser is, however, used as a heterodyne source. (The FID signal radiates at the original laser frequency.) Thus the mathematical description is split into two distinct time domains. We must calculate the time evolution of the system up to $t=\tau$ and then use this result as initial conditions for the free decay after $t=\tau$.

Using the above results, equations of motion for a two-level system in the presence of the radiation field are

$$\dot{\rho}'_{aa} = -i(\mu\cdot\mathcal{E}/\hbar)\cos\omega t\,(\rho'_{ab}-\rho'_{ba}) - \rho_{aa}/T_1\,, \tag{7a}$$

$$\dot{\rho}'_{bb} = -i(\mu\cdot\mathcal{E}/\hbar)\cos\omega t(\rho'_{ba}-\rho'_{ab})\,, \tag{7b}$$

$$\dot{\rho}'_{ab} = -i\omega_0\rho'_{ab} - i(\mu\cdot\mathcal{E}/\hbar)\cos\omega t\,(\rho'_{aa}-\rho'_{bb}) - \rho'_{ab}/T_2\,. \tag{7c}$$

The phenomenological relaxation times T_1, T_2 have been added, and for collisionless conditions $T_2 = 2T_1$. Because the Franck–Condon progression is usually extended over a wide frequency distribution, only the emission to levels other than $|b\rangle$ is considered. Also, since the only decay channel is a radiative one, the lower state relaxation is ignored because the radiative decay rate of this state is essentially zero. In prior work[18] on beams it was assumed that lower state relaxation is large enough to cause thermal equilibrium and hence to allow the application of conventional Bloch equations to beam transients. In our opinion this cannot be the case at zero pressure since there are no collisions in the beam to introduce equilibrium among the molecular levels.

Using the above conditions and converting Eq. (4) to the rotating frame with $\Delta = \omega - \omega_0$, the following equations are used for describing the transients in the beam which now represent an "open" system:

$$r_1 = \rho_{ba} + \rho_{ab}\,, \tag{8a}$$

$$r_2 = i(\rho_{ab} - \rho_{ba})\,, \tag{8b}$$

$$r_3 = \rho_{aa} - \rho_{bb}\,, \tag{8c}$$

$$r_4 = \rho_{aa} + \rho_{bb}\,. \tag{8d}$$

The corresponding Bloch equations are therefore given by

$$\dot{r}_1 = \frac{-1}{2T_1}\,r_1 + \Delta r_2\,, \tag{9a}$$

$$\dot{r}_2 = -\Delta r_1 - \frac{1}{2T_1}\,r_2 + (\mu\cdot\mathcal{E}/\hbar)\,r_3\,, \tag{9b}$$

$$\dot{r}_3 = -(\mu\cdot\mathcal{E}/\hbar)\,r_2 - \frac{1}{2T_1}\,r_3 - \frac{1}{2T_1}\,r_4\,, \tag{9c}$$

$$\dot{r}_4 = \frac{-1}{2T_1}\,r_3 - \frac{1}{2T_1}\,r_4\,. \tag{9d}$$

Note that amidst the algebra in proceeding from Eqs. (7) to (9) we have lost the time dependence of the field, a result of employing the rotating wave approximation. The above equations are just the analog to the FVH equations for a two-level system that is not closed. Thus for a given initial condition the population of the two levels approaches zero in time, i.e., $r_4 \to 0$, as $t \to \infty$. This last phenomenon is a manifestation of optical pumping[30] in a collisionless environment. We now proceed to solve Eqs. (9) by the Laplace transform method. Only r_1 and r_2 will be considered since the macroscopic polarization is determined by these quantities [Eq. (5)]. Rewriting the equations in a matrix form,

$$\dot{\mathbf{r}}(t) = \begin{pmatrix} -1/2T_1 & \Delta & 0 & 0 \\ -\Delta & -1/2T_1 & \mu\cdot\mathcal{E}/\hbar & 0 \\ 0 & -\mu\cdot\mathcal{E}/\hbar & -1/2T_1 & -1/2T_1 \\ 0 & 0 & -1/2T_1 & -1/2T_1 \end{pmatrix} \cdot \mathbf{r}(t)$$

$$= \mathbf{C}\cdot\mathbf{r}(t)\,, \tag{10}$$

where

$$\mathbf{r}(t) = \begin{pmatrix} r_1(t) \\ r_2(t) \\ r_3(t) \\ r_4(t) \end{pmatrix}\,. \tag{11}$$

The transform of $\mathbf{r}(t)$ is defined as

$$\mathbf{r}^T(S) = \int_0^\infty e^{-st}\mathbf{r}(t)\,dt \tag{12}$$

so that our equations become

$$(S\mathbf{I}-\mathbf{C})\cdot\mathbf{r}^T(S)=\mathbf{r}(t'), \tag{13}$$

where $\mathbf{I}$ is a unit matrix. The initial conditions at t' are taken as

$$\mathbf{r}(t')=\begin{pmatrix}0\\0\\-1\\+1\end{pmatrix}, \tag{14}$$

i.e., all the population is in the ground state.

Defining $S\mathbf{I}-\mathbf{C}\equiv\mathbf{A}$ gives

$$\mathbf{A}\cdot\mathbf{r}^T(S)=\mathbf{r}(t'). \tag{15}$$

Applying Cramer's rule, one obtains the following expressions for $r_1^T(S)$ and $r_2^T(S)$:

$$r_1^T(S)=-\Delta(\mu\cdot\mathcal{E}/\hbar)(S+1/T_1)/\det\mathbf{A} \tag{16}$$

and

$$r_2^T(S)=-(\mu\cdot\mathcal{E}/\hbar)(S+1/2T_1)(S+1/T_1)/\det\mathbf{A}. \tag{17}$$

By noting the equality of the diagonal elements of $\mathbf{A}$ we may factor its determinant, which yields

$$\det\mathbf{A}=(S+1/2T_1-\lambda^-)(S+1/2T_1+\lambda^-)\times(S+1/2T_1+i\lambda^+)(S+1/2T_1-i\lambda^+), \tag{18}$$

with

$$\lambda^{\pm}=\left[\left\{\tfrac{1}{4}[(\mu\cdot\mathcal{E}/\hbar)^2+\Delta^2-(1/2T_1)^2]^2+[\Delta/2T_1]^2\right\}^{1/2}\pm\tfrac{1}{2}\left\{(\mu\cdot\mathcal{E}/\hbar)^2+\Delta^2-(1/2T_1)^2\right\}\right]^{1/2}. \tag{19}$$

The Mellin inversion integrals may now be easily performed:

$$r_1(t)=(i/2\pi)\,\Delta(\mu\cdot\mathcal{E}/\hbar)\int_C[(S+1/T_1)/\det\mathbf{A}]e^{S(t-t')}\,ds$$

$$=\frac{-\Delta(\mu\cdot\mathcal{E}/\hbar)}{(\lambda^+)^2+(\lambda^-)^2}\,e^{-(t-t')/2T_1}\left\{\cosh\lambda^-(t-t')+\frac{1}{2T_1\lambda^-}\sinh\lambda^-(t-t')-\cos\lambda^+(t-t')-\frac{1}{2T_1\lambda^+}\sin\lambda^+(t-t')\right\}, \tag{20}$$

where C is a suitable contour which lies to the right of all singularities of the integrand in the complex plane. Similarly,

$$r_2(t)=-\frac{(\mu\cdot\mathcal{E}/\hbar)}{(\lambda^-)^2+(\lambda^+)^2}\,e^{-(t-t')/2T_1}\left\{\frac{1}{2T_1}\cosh\lambda^-(t-t')+\lambda^-\sinh\lambda^-(t-t')-\frac{1}{2T_1}\cos\lambda^+(t-t')+\lambda^+\sin\lambda^+(t-t')\right\}. \tag{21}$$

We now wish to compute the r_1 and r_2 components for a molecule with a particular velocity component v_y and positioned in front of the detector at time t. Referring to Fig. 3, the edges defining the detector width along the y axis are located at distances $y=l_1$ and $y=l_2$, respectively, where l_2-l_1 is the detector width. For a detector size of practical interest its length along the x axis will enter the problem only as a multiplicative constant determining the overall signal strength. That is, this length parameter reflects only the total number of molecules being sampled but does not affect the dynamics. Assuming that the origin of the coordinate system lies at the position where the molecules enter the left edge of the laser beam, then a molecule with velocity v_y located at $y=l$ with $l_1<l<l_2$ has been in the laser field for time l/v_y. Thus, to calculate $r_1(t,t')$ (we add an argument to denote the time where initial conditions apply) for this molecule we merely assert that $t-t'=l/v_y$ and apply our previous solutions. Setting t equal to zero, since later this will be the time at which the laser is removed or frequency shifted, we obtain

$$r_1\left(t=0,\frac{-l}{v_y},\Delta\right)=-\frac{\Delta(\mu\cdot\mathcal{E}/\hbar)}{(\lambda^+)^2+(\lambda^-)^2}\,e^{-l/2T_1v_y}\left\{\cosh\lambda^-\frac{-l}{v_y}+\frac{1}{2T_1\lambda^-}\sinh\lambda^-\frac{-l}{v_y}-\cos\lambda^+\frac{l}{v_y}-\frac{1}{2T_1\lambda^+}\sin\lambda^+\frac{l}{v_y}\right\} \tag{22}$$

and a similar equation for $r_2(t=0,\ -l/v_y,\ \Delta)$. The detuning parameter is denoted explicitly for this particular molecule.

The analysis for the first time domain is now completed, that is, the preparation of molecules by the laser field at ω. To proceed involves the designation of $t=0$ as the point in time at which the light at ω is removed. The equations of motion in this time region are those of (9) with $\mu\cdot\mathcal{E}=0$. Now the time development is straightforward, giving

$$r_1(t)=\left[r_1\left(0,\frac{-l}{v_y},\Delta\right)\cos\Delta t+r_2\left(0,\frac{-l}{v_y},\Delta\right)\sin\Delta t\right]e^{-t/2T_1}, \tag{23}$$

$$r_2(t)=\left[r_2\left(0,\frac{-l}{v_y},\Delta\right)\cos\Delta t-r_1\left(0,\frac{-l}{v_y},\Delta\right)\sin\Delta t\right]e^{-t/2T_1}. \tag{24}$$

As shown in Eq. (6) the electric field amplitude corresponding to a free induction decay signal is related to the polarization [Eq. (5)] which is explicitly given by (23) and (24) in the beam. At this point the ensemble averaged $r_1(t)$ and $r_2(t)$ must be constructed. This is accomplished by the following scheme. First it is recognized that an effusive molecular beam displays the thermal properties of its oven source, thus the ensemble distribution function for the y component of velocity is just Boltzmann. Secondly, one must account for the Doppler broadening of the transition resonance by the distribution of velocity components v_z. Molecules moving with v_z exhibit an effective transition frequency of $\omega_0=\omega_D(1+v_z/c)$, where ω_D is the inherent frequency or the location of the peak of the Doppler broadened

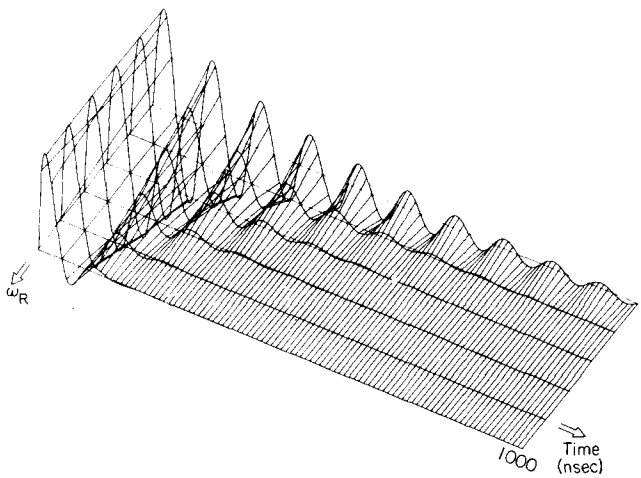

FIG. 4. The FID signal as a function of time and the Rabi frequency, $\omega_R = \mu \cdot \mathcal{E}/\hbar$. The Rabi frequency is 2, 4, 6, 10, 15, and 20 MHz, respectively. The beats are due to the heterodyne method of detection. The laser switching frequency is 10 MHz and $T_2 = 2.5$ μsec. The first peak of the signal is normalized for all the different $\mu \cdot \mathcal{E}$ values. Note that as ω_R increases the FID rate is getting larger. Temperature is 273 K and $L = 0.1$ cm.

transition. (The speed of light is c.) Thus if the laser is on resonance with the Doppler peak, $\omega = \omega_D$, then $\Delta = -v_z\omega_D/c$. Again v_z is described by a simple Boltzmann distribution.[31] Finally, there is one additional integral. Since the detector sees those molecules from $y = l_1$ to $y = l_2$, a spatial average must be performed. The detector width is assumed small enough to ignore the variation of molecular density with l caused by the diverging molecular beam. The resulting field is denoted as $\overline{\mathcal{E}_{\rm FID}}$. We therefore have

$$\overline{r_2(t)} = \bar{n}k_0 e^{-t/2T_1}\int_0^\infty dv_y \int_{-\infty}^{\infty} d\Delta \int_{l_1}^{l_2} dl\, e^{-v_y^2 c_0 - \Delta^2 c_1} \otimes\left[r_2\left(0, \frac{-l}{v_y}, \Delta\right)\cos\Delta t - r_1\left(0, \frac{-l}{v_y}, \Delta\right)\sin\Delta t\right], \tag{25}$$

where $c_0 = \frac{1}{2}m/kT$, $k_0 = \frac{1}{2}(m/\pi kT)(c/\omega_D)$, $c_1 = \frac{1}{2}(c/\omega_D)^2 \times (m/kT)$, and $\bar{n}$ is the number of molecules per unit length in front of the detector. The constants in Eq. (25) are the usual Boltzmann constants. The corresponding integrals for r_1 vanish owing to the symmetry of the integrand as a function of Δ. So with $\bar{r}_1(t) = 0$ the field is given by

$$\overline{\mathcal{E}_{\rm FID}(t)} \simeq \frac{\omega L\eta}{2c\epsilon}(\mu\,\overline{r_2(t)}) = \frac{i\omega L\eta}{c\epsilon}\,\mu\,\bar{\rho}_{ab} \tag{26}$$

Molecular propagation effects across the detector in the free decay time regime have been ignored, so the equations are valid provided

$$2T_1 V_{\rm rms} \ll l_2 - l_1 = L\,. \tag{27}$$

This inequality is satisfied experimentally.

A. Effect of power broadening and transit time

Figures 4 and 5 show the solution [Eq. (26)] for the FID signal at various values of $\mu \cdot \mathcal{E}$. The v_y and Δ integrals of Eq. (25) were done numerically with values of the remaining parameters consistent with our experiments performed on the $X^1\Sigma_g^+ \rightarrow B^3\Pi_{0^+u}$ transition of I_2 at 5897.5 Å. The dephasing time is taken to be $T_2 = 2T_1 = 2.5$ μsec from the measured value of T_1 as described later. The approximate oven temperature and the detector width are given in the experimental section. The computer plots show the heterodyne beats due to the detection method at a switching frequency of 10 MHz. Thus the depicted transient signals are relatively small in magnitude and are situated on a large dc background which is not shown.

Figure 4 shows the decay behavior of the FID, with the transient peaks normalized to the same value, as $\mu \cdot \mathcal{E}/\hbar = \omega_R$ (Rabi frequency) is varied. Figure 5 gives the actual relative magnitudes of the signal as a function of ω_R. For both graphs the vertical axis is the intensity of the signal in arbitrary units and the gradations denote equi-intensity contours. The time axes are linear.

Several observations can be made at this point. The effect of increasing the laser power is to increase the apparent rate of decay. In fact, the high $\mu \cdot \mathcal{E}$ range [relative to $(1/T_2)$] is characterized by decay rates which go linearly with $\mu \cdot \mathcal{E}$ and it is in this limit that FID measurements are not particularly useful. In this regime, contributions to the decay rate by the interesting molecular processes ($1/T_2$ contributions) are masked by the dominant power saturation effects. The origin of these effects is somewhat evident. A Doppler dephasing (and therefore decay) is experienced because the spread of molecular frequencies contributing to the FID get out of phase. Since increasing the laser power increases the spread of frequencies the dephasing time shortens for this contribution. As we have mentioned, this effect is well known from past FID work on gases. However, the details of the effect are altered somewhat when making the measurement using the molecular beam. This is illustrated by the example shown in Fig. 6 which contains two transients characterized by identi-

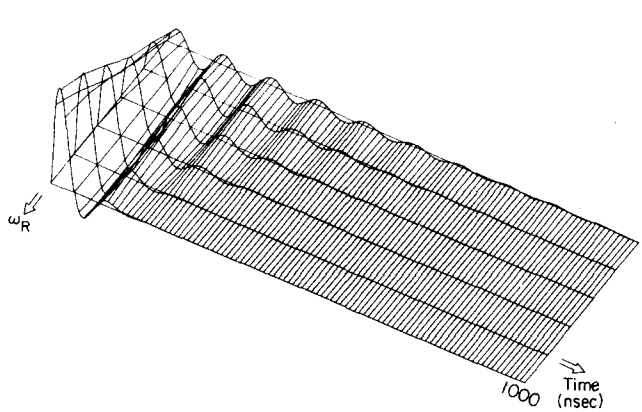

FIG. 5. The actual FID signal as a function of time and the Rabi frequency, $\omega_R = \mu \cdot \mathcal{E}/\hbar$. The Rabi frequency is 2, 4, 6, 10, 15, and 20 MHz, respectively. The beats are due to the heterodyne method of detection. The laser switching frequency is 10 MHz, and $T_2 = 2.5$ μsec. The signal is not normalized as in Fig. 4. Note that as ω_R increases the FID rate gets larger but the size of the signal increases.

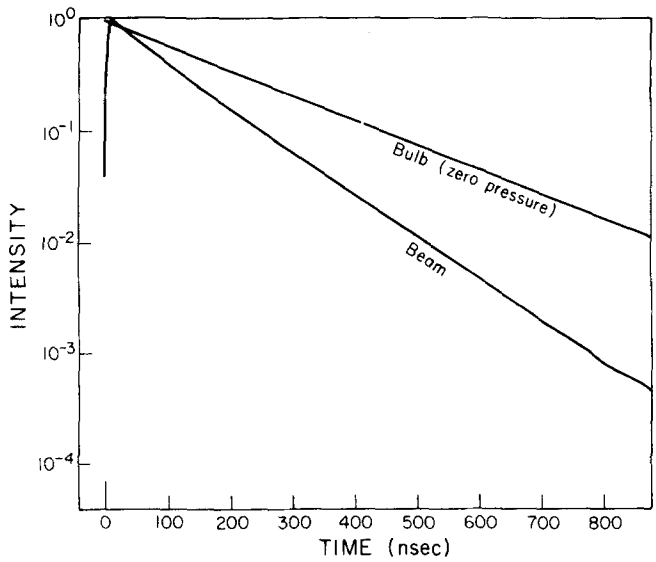

FIG. 6. Comparison between beam results obtained from the theory presented in this paper and bulb results extrapolated to the zero pressure limit. The decay, although close to exponential is not a perfect one. $\omega_R = 6$ MHz, $L = 0.1$ cm, and $T = 273$ K.

cal parameters. (We have not included the beats on these curves to help clarify the comparison.) The upper graph is the result of the zero pressure extrapolation of the conventional theory[26] which provides the following expression for the FID:

$$\frac{1}{\tau} = \frac{1}{T_2} + \frac{1}{T_2}[1 + (\mu \cdot \mathcal{E}/\hbar)^2 T_1 T_2]^{1/2} . \tag{28}$$

The lower graph represents the theory as adopted to molecular beam work which we have just presented. We note that while the total rate $1/\tau$ of Eq. (28) is linear in $\mu \cdot \mathcal{E}$ at large values of $\mu \cdot \mathcal{E}$ this expression is not applicable to the current problem as Fig. 6 indicates ($\mu \cdot \mathcal{E}/\hbar = 6$ MHz). Equation (28) was derived for a

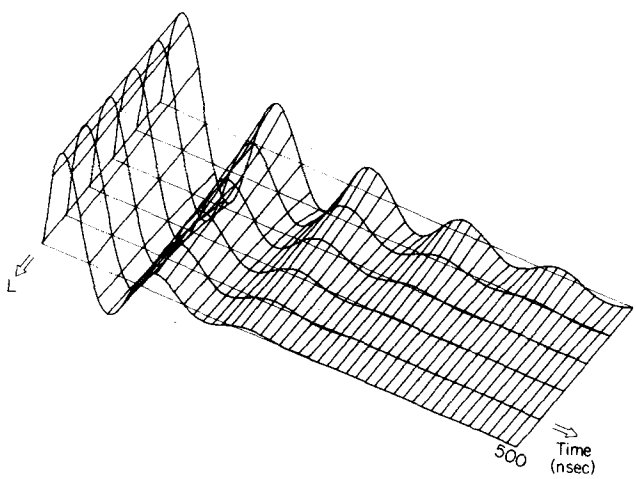

FIG. 7. Effect of detector width on the FID signal. The plot shows the signal as a function of time and L. In this figure the detector has its origin at the beginning of the laser and continues for a finite length (see Fig. 3). The lengths are 0.1, 0.3, 0.5, 0.7, 0.9, and 1.1 cm. Note that as L increases the FID rates get larger. Plots of the decay time vs the detector width show near logarithmic dependence. $\omega_R = 4$ MHz.

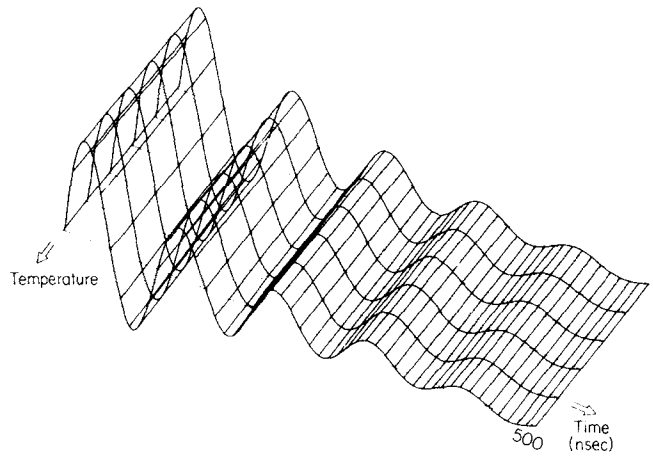

FIG. 8. Effect of oven (or container) temperature on the beam FID. The plot shows the dependence of the signal on time and temperature; 0, 10, 20, 30, 40, and 50°C. Essentially there is no change in the decay characteristics of the beam $\omega_R = 4$ MHz and $L = 0.1$ cm.

closed ensemble which as mentioned before will not adequately describe the beam case. Even if the decay constant of Eq. (28) agrees with that obtained from the beam theory for certain values of detector size, the interpretation is unphysical for the reasons given above (see also Appendix A). It is interesting to note from the results of Sec. C and the Appendix that at very low powers the decay of the signal in bulbs and in beams is simply given by T_1. This means that the laser intensity is low enough that the steady state preparation and the velocity averaging is not altering the decay characteristics.

B. Effect of beam temperature and detector geometry

Figure 7 illustrates the dependence of the FID signal upon detector width L at a fixed l_1 with the transient peaks normalized to the same height. It is clear that the decay rate manifests a drastic L dependence which could pose serious problems during the precise measurement of molecular parameters. However, as we shall discuss in Sec. C, this problem can be eliminated if low enough power is utilized in the experiments. In Fig. 7, the detector edge has its origin at the beginning of the laser, and the detector length is varied from 0.1 cm to 1.1 cm. An essentially linear dependence for the log of the decay constant on the detector width was found. In Fig. 8, we show the solution of beam equations as a function of temperature, again with normalized peak heights. Essentially there is no change over the range 0 °C to 50 °C. This is not surprising in light of the fact that the Doppler width in this temperature range is much larger than the homogeneous linewidth of the transition. In other words, varying this parameter merely adjusts the distribution widths used in performing ensemble averages. Though the dependence seems very slight, caution must be exercised in any experimental verification of this point since increasing temperature also decreases the mean free path within the oven (or the container). Thus for a given oven slitwidth the molecular beam may lose its effusive properties unless $\lambda \gg \delta$, where λ is the mean free path and δ is the slitwidth.

C. Analytical solutions: the low power limit

The expression for $\bar{r}_2(t)$ contains three integrations, of which only the l integration could be done explicitly. The remaining integrations have been performed numerically for a variety of interesting parameters, as discussed before. To obtain analytical solutions we will consider cases where the experiments are done in the low power regime and/or at several power levels. In the latter case, the decay time of the FID is taken to be the zero power extrapolated value. First we perform the l integral which gives (with $t' = l/v_y$),

$$\bar{r}_2(t) = e^{-t/2T_1}\int_0^\infty dv_y \int_{-\infty}^{\infty} d\Delta[F_2(v_y,\Delta)\cos\Delta t - F_1(v_y,\Delta)\sin\Delta t]\otimes e^{-v_y^2 c_0} e^{-\Delta^2 c_1} k_0\bar{n} \tag{29}$$

with

$$F_2(v_y,\Delta) = -\frac{1}{2}\frac{(v_y\mu\cdot\mathcal{E}/\hbar)}{(\lambda^+)^2+(\lambda^-)^2} e^{-t'/2T_1}\left[\frac{(\lambda^- + 1/2T_1)}{(\lambda^- - 1/2T_1)} e^{\lambda^- t'} + \frac{(\lambda^- - 1/2T_1)}{(\lambda^- + 1/2T_1)} e^{-\lambda^- t'}\right]\Bigg|_{t_1}^{t_2}, \tag{30}$$

$$F_1(v_y,\Delta) = -\frac{1}{2}\frac{v_y\Delta\mu\cdot\mathcal{E}/\hbar}{(\lambda^+)^2+(\lambda^-)^2} e^{-t'/2T_1}\left[\frac{(\lambda^- + 1/2T_1)}{(\lambda^- - 1/2T_1)\lambda^-} e^{\lambda^- t'} - \frac{(\lambda^- - 1/2T_1)}{(\lambda^- + 1/2T_1)\lambda^-} e^{-\lambda^- t'}\right]\Bigg|_{t_1}^{t_2}. \tag{31}$$

Terms which oscillate at frequency λ^+ have not been kept as one can show that their contributions to the remaining integrals are small for $\mu\cdot\mathcal{E}/\hbar \ll 1/2T_1$ and $\mu\cdot\mathcal{E}/\hbar \gg 1/2T_1$. This is due in part to the relative magnitude of the coefficients of these terms compared to the ones we have kept. Complications involved in the remaining integrals originate primarily from the form of $\lambda^\pm$. We avoid these problems by successively expanding the square roots of $\lambda^\pm$ for $(\mu\cdot\mathcal{E}/\hbar)/(1/2T_1)^{-1} \ll 1$. Rewriting $\lambda^\pm$ gives

$$\lambda^\pm = \left[\left\{\frac{1}{4}\left[\left(\frac{\mu\cdot\mathcal{E}}{\hbar}\right)^2 + \Delta^2 + \left(\frac{1}{2T_1}\right)^2\right]^2 - \left[\frac{\mu\cdot\mathcal{E}}{2\hbar T_1}\right]^2\right\}^{1/2} \pm \left\{\frac{1}{2}\left[\left(\frac{\mu\cdot\mathcal{E}}{\hbar}\right)^2 + \Delta^2 - \left(\frac{1}{2T_1}\right)^2\right]\right\}\right]^{1/2}. \tag{32}$$

The expansions described above yield

$$\lambda^- \simeq \frac{1}{2T_1}\left(1 - \frac{1}{2}\frac{(\mu\cdot\mathcal{E}/\hbar)^2}{\Lambda}\right), \tag{33a}$$

$$(\lambda^+)^2 + (\lambda^-)^2 \simeq \Lambda - 2(\mu\cdot\mathcal{E}/\hbar)^2(1/2T_1)^2\Lambda^{-1}, \tag{33b}$$

$$\Lambda = \Delta^2 + (\mu\cdot\mathcal{E}/\hbar)^2 + (1/2T_1)^2. \tag{33c}$$

Substituting the above expressions into Eqs. (30) and (31) and retaining only lowest order terms we get

$$F_1 = \left[\frac{2v_y\Delta}{(\mu\cdot\mathcal{E}/\hbar)(1/2T_1)}\frac{\exp\{-\frac{1}{2}(\mu\cdot\mathcal{E}/\hbar)^2(1/2T_1)lv_y^{-1}\Lambda^{-1}\}}{(1-2(\mu\cdot\mathcal{E}/\hbar)^2(1/2T_1)^2\Lambda^{-2})} - \frac{1}{8}\frac{v_y\Delta(\mu\cdot\mathcal{E}/\hbar)^3}{(1/2T_1)}\frac{\exp\{-2(1/2T_1)lv_y^{-1}\}}{(\Lambda^2 - 2(\mu\cdot\mathcal{E}/\hbar)^2(1/2T_1)^2)}\right]\Bigg|_{t_1}^{t_2}. \tag{34}$$

Similarly, for F_2 we compute

$$F_2 \simeq \left[\frac{2v_y}{(\mu\cdot\mathcal{E}/\hbar)}\frac{\exp\{-\frac{1}{2}(\mu\cdot\mathcal{E}/\hbar)^2(1/2T_1)lv_y^{-1}\Lambda^{-1}\}}{(1-2(\mu\cdot\mathcal{E}/\hbar)^2(1/2T_1)^2\Lambda^{-2})} + \frac{v_y}{8}\frac{(\mu\cdot\mathcal{E}/\hbar)^3 e^{-l/T_1 v_y}}{(\Lambda^2 - 2(\mu\cdot\mathcal{E}/\hbar)^2(1/2T_1)^2)}\right]\Bigg|_{t_1}^{t_2}. \tag{35}$$

After the integration over v_y and Δ, and keeping the lowest order terms in $(\mu\cdot\mathcal{E}/\hbar)$ we get the following expression (see Appendix A) for $\overline{r_2(t)}$:

$$\overline{r_2(t)} \simeq A\, e^{-t/T_1}, \tag{36}$$

where A is a constant which depends on $\mu\cdot\mathcal{E}$ and the width of the detector.

The last result is gratifying for several reasons. Not only do we recover the expected low power limit expression for the temporal decay of the FID for a bulb environment $1/\tau = 1/T_1$, but it is shown that this power regime is characterized by a decay time that is independent of the detector slitwidth and other geometrical parameters. The implications of the latter result are clear: the conditions described in the preceding are sufficient to alleviate apprehension that the particular experimental geometry influences the FID decay rate. It should be noted that the above conclusions apply only to the low power case. For large $\mu\cdot\mathcal{E}$ values the situation is different. This is demonstrated by numerically computing the v_y and Δ integrations after explicitly doing the l integral as before (see Sec. A and B).

III. EXPERIMENTAL

The molecular beam apparatus with which the FID on iodine was observed is shown schematically in Fig. 9. The entire apparatus was initially baked out and the purified iodine was placed in the oven section of the apparatus. The iodine effusively passes through a narrow (200 μ) slit. Close to it the laser excites the molecular beam. This chamber where the laser and the molecular beams are interacting in a perpendicular geometry is evacuated by diffusion and cryopumping. The oven is either at room temperature or at ~40 °C above room temperature. As mentioned before, the precise temperature of the oven is not crucial to the decay charac-

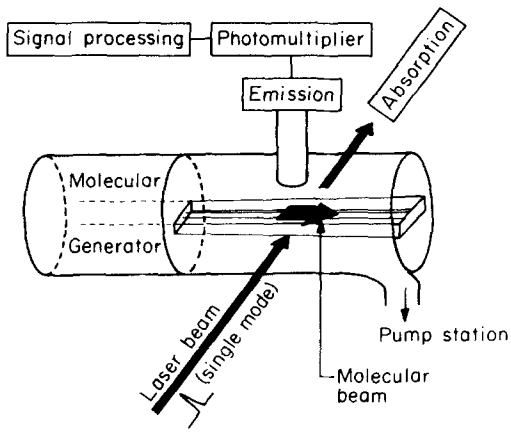

FIG. 9. A schematic for the geometrical arrangement used in our beam-laser experiments. The absorption in the forward direction gives the coherent transients which appears as a heterodyne signal. The emission at right angles to the laser beam gives both the incoherent and coherent resonance decay of the molecules in the beam.

teristics (provided the flow remains effusive) though it is very critical in determining the signal intensity. The collisionless nature of the molecular beam was checked by comparing the T_1 decay in the beam to the zero pressure extrapolated value of the Stern–Volmer plot in the bulb. Excellent agreement was found. However, this is a less sensitive test of the collisional quality of the beam than that obtained by comparing the value of T_2 extracted from FID and T_1 from the spontaneous decay.

A modified 580 A spectra physics dye laser (rhodamine-6G in ethylene glycol) pumped by a cw argon ion laser (total power 18 W) provided the single mode excitation source. The quality of the single mode was monitored by a scanning Fabry-Perot interferometer which showed a rms frequency jitter of approximately 6 MHz for long scan times. The amplitude of the dye laser was stabilized during the experiments (to $\pm 0.5\%$ at a fixed wavelength) using a feedback loop to the argon ion laser. The single mode selects the ro-vibronic state at 5897.46 Å ($v'' = 2$, $J'' = 59$ to $v' = 15$, $J' = 60$) of the electronic origin $X\,^1\Sigma_g^+ \rightarrow B\,^3\Pi_{0^+u}$.

Inside the dye laser cavity we inserted an AD*P crystal to utilize as as electro-optic element (disperion = 60 MHz/100 V) for switching the laser frequency.[32] This way the transients can be observed either in the forward direction[32,6–8] of the laser or on the emission spectra at right angles[6,7] to the exciting beam.

For the forward coherent signal we have used a photodiode (active area $= 2.0 \times 10^{-3}$ cm^2) in connection with a low-noise amplifier and a sampling scope (or a box car integrator, PAR Model 162). For the emission detection an EMI (Model 9558) photomultiplier was used. After eliminating the exciting light, the emission was focused on the photocathode and the output of the photomultiplier was processed to obtain the transients. In all these experiments the frequency of the transition was measured by a high resolution spectrometer. The power density of the single-mode laser (up to 18 W cm^{-2}) was measured using a thermopile (Scientech Model 360001) and a pair of slits. The latter was used to scan the laser transversely in order to determine the width of its (excellent) Gaussian profile.

IV. RESULTS AND DISCUSSION

To obtain the FID of iodine beam the single mode of the laser was tuned to the molecular resonance by optimizing the emission. The switching of the laser was then performed by feeding a voltage pulse (typically 2 μsec) to the AD*P crystal inside the cavity.

In the crossed zone of molecular and laser beams, the resonant molecules (i.e., $\omega = \omega_0$) were coherently excited by the laser, and a steady state value for the r vector was established. Switching the laser into new frequency (say ω') the prepared steady state coherence of the ω_0 molecules decays freely, while the ω' molecules absorb the switched laser light and undergo optical nutation. At low enough powers, the ω' molecules will not absorb much light and they become essentially transparent (i.e., no nutation). Thus the transmitted beam at ω' will beat with the superradiant field emitted at ω_0 when the total signal is registered on a square-law detector (heterodyne detection). Naturally, the beat frequency is determined by the switching frequency which in turn is determined by the dispersion of AD*P crystal.

Figure 10 depicts the observed (continuous beat pattern) FID in iodine beam. The top signal was seen when the laser was switched 6 MHz away from the pump frequency. The bottom spectrum was taken at higher switching frequency, 12 MHz. As expected the heterodyne beat frequency follows the switching frequency.

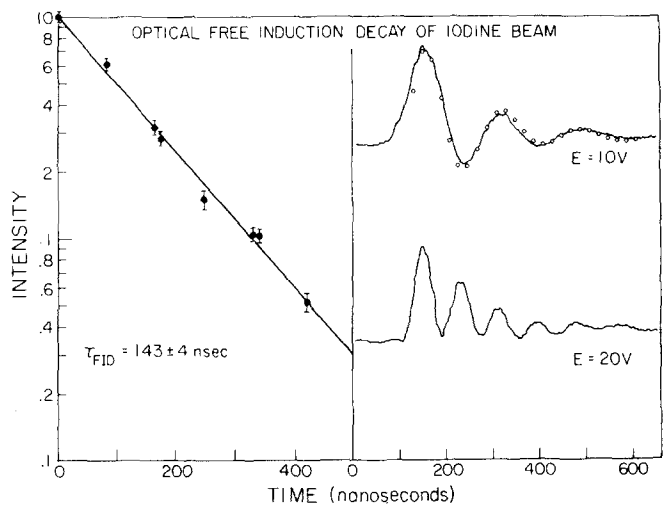

FIG. 10. The optical FID observed in an iodine beam excited with the single mode of the laser at 5897.5 Å. As shown in the figure, the beat frequency follows the electro-optic switching frequency (10 and 20 V). The open circles in the top-right transient spectrum gives the theoretical curve obtained from Sec. III; the period is 163.4 nsec and the decay time constant (144.3 nsec) is in good agreement with the experimental value. The drawing on the left shows the exponential decay of the signal within our experimental errors.

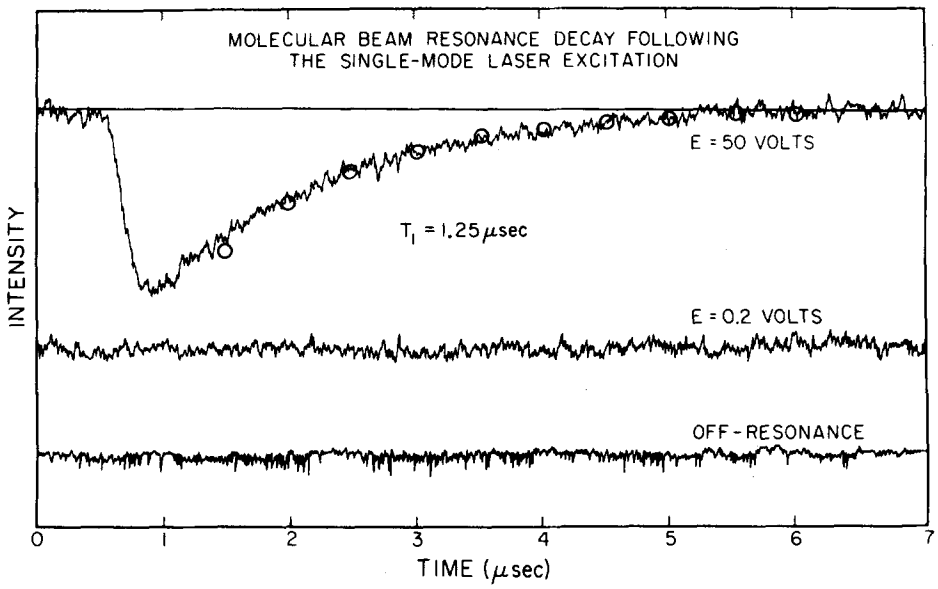

FIG. 11. The right-angles resonance decay of coherently excited (single-mode) iodine beam. The top two traces were taken with an electro-optic voltage of 50 and 0.2. The bottom trace was taken when the laser was off resonance with the beam transition (width = 123 kHz). In these experiments care was taken to completely shield the emission from the exciting beam. The open circles are the theoretical points which give a T_1 decay constant of 1.25 μsec.

This figure[8] is presented for comparison with theory.

The left section of Fig. 10 shows the exponentiality of the FID. The decay constant is $\tau = 143 \pm 4$ nsec. Utilizing Eq. (26), similar graphs to that of Fig. 5 were obtained for the case under study. We fed the experimental data to the computer and obtained the best fit shown by the open circles superimposed on the experimental data in Fig. 10. The fit provides a more accurate description than the preliminary analysis used in the early work (I).

The theory provides the Rabi frequency $\omega_R = 4.9$ MHz and a beat period of 163.4 nsec. Further, the theoretical decay time constant is 144.3 nsec, which is very close to the measured decay time constant (143 ± 4 nsec). Although the theory is in good agreement with the experiments and is consistent with the condition of the beam requirement (i.e., $T_2 = 2T_1$), the uncertainty in obtaining the dephasing time directly is large owing to power broadening. We have attempted to measure ω_R directly in the molecular beam, but a nutation signal was not detected. Instead, we have used the FID and the nutation in an iodine bulb and scaled the obtained ω_R in the bulb by the new laser power used in the beam experiment. [The FID of the bulb follows the prediction of Eq. (28), and again the beat frequency is the switching frequency.] Although by this approach we obtained a reasonable agreement between the computed ω_R and the theoretical value, it is difficult to know the exact laser power density that the crossed laser and molecular beams zone sees. Moreover, to test the theory further we need to know the decay at relatively low powers. This problem will be circumvented in the future by using the echo emission techniques,[7] and by enhancing our sensitivity to measure the FID at low powers. Note that the theory presented in this paper is applicable to transients decaying at any power level.

The emission at right angles to the laser and molecular beams gives the signal shown in Fig. 11 for different switching frequencies. Switching the laser from ω_0 to ω' we expect to see a spontaneous emission from the ω_0 molecules (T_1 decay) and a nutation from the ω' molecules. Thus the photomultiplier which monitors the total emission should show a decay with beats (frequency = ω_R) on the top of it. However as discussed elsewhere (see Paper I), the nutation signal is weak and damps out fast, and only for the transients with very high S/N can we observe these beats on the T_1 decay.[9] The purpose of showing the T_1 decay is to gauge the collisionless quality of the beam we used for the FID measurement. The best theoretical fit gives $T_1 = 1.25$ μsec, which agrees well with the zero pressure value of 1.29 ± 0.5 μsec obtained from the Stern–Volmer plot for iodine in a bulb. Furthermore, by combining the results of the FID and the T_1 decay, one concludes that the homogeneous width of the transition is 123 kHz in the beam. It is interesting to note that when the switching voltage on the AD*P crystal was 0.2 V there was no transient signal. This voltage corresponds to a shift frequency of 120 kHz, i.e., the laser did not shift out of the homogeneous line and therefore one does not expect any transients to appear on the detector as shown in Fig. 11.

The laser power needed to produce $\pi/2$ pulses can be calculated using the results of Eq. (3) which gives the probability of finding the molecule in the excited state. In the absence of relaxation, this probability can be rewritten in the following form (on resonance):

$$\rho'_{aa}(t) = \tfrac{1}{2}[1 - \cos(\mu \cdot \mathcal{E}/\hbar)t] = \sin^2(\mu \cdot \mathcal{E}/2\hbar)t\,. \tag{37}$$

To cause a saturation in the lwo-level system, the Rabi frequency will be related to time by

$$\omega_R = (\mu \cdot \mathcal{E}/\hbar) = \pi/2t\,, \tag{38}$$

where t is the time spent by the molecule in the laser beam. The laser power can be calculated using the time averaged Poynting vector,

$$\langle |S| \rangle = (c/8\pi)|\mathcal{E}|^2\,. \tag{39}$$

Combining Eqs. (38) and (39), we obtain

$$\langle|S|\rangle = (\pi\hbar^2 c/32)(t\mu)^{-2}, \tag{40}$$

which gives

$$\langle|S|\rangle = 3.3\times10^{-16}(t\mu)^{-2}. \tag{41}$$

In Eqs. (41), the transition moment is in debyes, time is in seconds, and S is in W/cm^2.

For an iodine beam we calculated an average velocity of 1.6×10^4 cm/sec. The transverse laser beam profile of Gaussian with a width $w=0.05$ cm. The total power is therefore

$$\begin{aligned} P &= \frac{c}{8\pi}\int_0^\infty \mathcal{E}^2(2\pi r)\,dr \\ &= \frac{c}{4}\int_0^\infty \mathcal{E}_0^2 e^{-r^2/w^2} r\,dr \\ &= 10.4\times10^{-16} w^2(\mu t)^{-2}. \end{aligned} \tag{42}$$

Since the iodine molecule spends on the average 3 μsec in the laser beam, then $P=0.11$ m W. In arriving at this conclusion we have used a μ of 0.05 D for the iodine transition at 5897.5 Å. The surprisingly low value of P is due to the long transit time, i.e., the $\pi/2$ pulse is on for very long time. Further, P depends quadratically on μ, which means that special care must be given in measuring μ in order to estimate the power reasonably well. The signal intensity also depends on the total number of molecules in the laser beam. This is particularly true for the nutation whose detection is not done by the heterodyne method of FID. One of the difficulties is that we cannot measure accurately the actual laser beam waist at the crossing zone with the molecular beam. This may be circumvented in the future.

Several points must be made before we conclude this section. First, the beam measurements provide a homogeneous linewidth of 123 kHz for the iodine transition. The laser effective bandwidth is small (< 1 MHz) such that there is no large loss in the signal amplitude. This point in fact made iodine beams very attractive devices for stabilizing cw dye lasers. Second, the above discussion considered two levels without relaxations in order to estimate the minimum laser power needed. If T_1 and T_2 are included then Eq. (37) cannot be used and one must solve the equations of motion as we did in previous sections. However, in the strong power limit, i.e., $\mu\cdot\mathcal{E}/\hbar \gg 1/T_1$, $1/T_2$, the results presented are valid. Third, the extension of the above treatment to off-resonance pumping is straightforward. In this case, the Rabi frequency ω_R will be replaced by $(\Omega=[\omega_R^2+\Delta^2]^{1/2})$ and the overall probability of finding the molecule in the excited state will have a Lorentzian term before the time-dependent term. Finally, in iodine within our large experimental error the only source for optical phase relaxation (2.5 μsec) is the spontaneous decay (1.25 μsec) at zero pressure in the molecular beam.

V. CONCLUSIONS AND COMMENTS

In this section we summarize our conclusions about optical T_1 and T_2, and their relationships to energy and phase randomization. The relevance of these relaxations to pure and seeded iodine beams will be discussed. Finally, we will comment and speculate about these processes in large molecules.

1. Energy randomization (by optical T_1 effects) and phase relaxation (by pure optical dephasing) are distinct and may play different roles in the dynamics of reactive or nonreactive molecular processes that follow the optical excitation. Optical dephasing times are usually short compared to T_1. This means that excitation of quasi stationary states (i.e., molecular eigenstates interacting, e.g., with the radiation field) by narrowband lasers might not lead into a narrow-energy distribution or a selective dissociation in molecules (see Fig. 1). As a result, during the T_1 process by which the population is depleted radiatively and/or nonradiatively, the excitation can sample a large energy region of the molecule. [This region might overlap with a large number of states in a repulsive well, thus giving nonselective chemistry.] Such cases will perhaps be more pronounced in large molecules where the density of excited final states is quite large. In small molecules the situation is different. From the work presented on iodine beams we now know that the spontaneous radiative decay time is $T_1=1.25$ μsec, and that this decay is the source for optical dephasing. In other words, in small molecules like diatomics in a beam $T_2=2T_1$ as shown in the theory section. Our measurements were done on a pure beam of iodine which is different from the now known van der Waals complexes of iodine with helium or argon, formed in free jet nozzles.[33] The optical dephasing in these complexes is different from pure iodine. In addition to the radiative decay to the ground state, there exist energy transfer channels which include the rearrangement of the van der Waals bond into an iodine vibrational excitation. We are now investigating the phase coherence associated with this bond breakage.

2. The ensemble averaging developed in this paper is not a velocity averaging like those developed by Ramsey[10] and by Klemperer *et al.*[14] for describing magnetic and electric cw resonances in beams. In our case we are investigating the time evolution of the population and the polarization induced by the laser. The complexity of the equations for describing r_1 and r_2 comes about because in beams the system is statistically open and the two-level equations of motion cannot be described by the simple Bloch vector. In fact, we have shown in this paper that the theoretical description developed for gas phase work in bulbs cannot directly apply to molecular beam circumstances. The appropriate modification of the traditional Bloch description was realized and interesting data concerning the FID in molecular beams were presented in numerical form

3. Molecular beam experiments on large molecules should provide different dephasing and T_1 relaxation times depending on the nature of the excitation source. In laser-induced emission from small molecules there are no problems regarding the measurement of T_1. This is because, although the molecules of different velocities have been prepared differently [Eq. (25)],

the decay is incoherent and takes place after the laser pulse is completely turned off. Note that the effect of transit broadening will not influence nearby levels provided the density of states is sufficiently low. For T_2 measurements the situation is entirely different because the coherent preparation determines the FID characteristics. Therefore the FID patterns in large molecules will depend on whether the laser prepares a coherent superposition or a statistical mixture of the molecular states.[1-4] In the former case the FID might exhibit two features in addition to the fast nonradiative dephasing at short times. Firstly, at longer times compared to the dephasing time (prior to which the molecular states are locked in phase) the molecular states will decay statistically. Secondly, genuine molecular beats are expected since the states will not fully lose their identity in the beam as they do by collisions in bulbs. In the case of preparing the molecular states statistically they will decay with their own time constant. The two limits of excitation depend on the laser bandwidth and coherence.[34] We therefore reach the following conclusions: (a) In analyzing coherent optical effects in beams of large molecules one must be careful not to relate the coherent decay to a dephasing process unless the laser characteristics (pulse width, frequency width, correlation time, etc.) are known and the ensemble *average* is done. Further, the method of excitation preparation (steady state vs pulsed experiments) is also important, as shown from our work[9] and the work of Jortner and Kommandeur[35]; (b) Under certain excitation conditions large molecules might act as being small (the sparse level structure limit), and the coherent coupling becomes that of the two-level system.[9,36] Thus the FID will exhibit the usual characteristics. Finally, (c) If the molecules in effusive beams are excited by broadband excitation, sequence congestion will result in the loss of phase coherence. This is because the excitation into the upper level carries a thermal distribution from the ground state. As pointed out by Jortner and Kommandeur,[35] one must utilize a density matrix formalism that is similar to that of Gordon *et al.*[37] used for describing the photon echo in SF_6. Because of this problem nozzles are superior to effusive sources, a fact which resulted recently in a new field of spectroscopy.[27] Experiments on the dephasing of pentacene and other molecules in supersonic jets are now under investigation in our laboratory.

Note added in proof: In a recent paper by Klemperer and his co-workers [J. Chem. Phys. 67, 4952 (1977)] an expression for the population of ground state molecules in a beam was derived by solving the time-dependent Schrödinger equation. Using our equations and identifying their $\omega - \omega_1$ as Δ, $\gamma/\hbar$ as $1/2T_1$ and $4b^2$ as $(\mu \cdot \epsilon/\hbar)^2$ we obtain an expression for the *population* [i.e., $(r_4 - r_3)/2$] that is identical to theirs. The procedure for obtaining r_4 and r_3 is similar to that outlined in Sec. II for obtaining r_1 and r_2. It is worth noting that the ensemble averaging procedure done on the r vector depends crucially on the geometry of the experiment. In their experiments, they averaged over the Doppler profile since they are dealing with optical transitions. In the rf region, however, the transit averaging is usually done following the classical procedure of Ramsey.

ACKNOWLEDGMENTS

Acknowledgment is made to the Donors of the Petroleum Research Fund, administered by ACS, for partial support of this research. This work was also supported in part by the Energy Research and Development Administration and partly by the Research Corporation. One of us (A.H.Z.) would like to thank Professor Don Levy of the University of Chicago for very stimulating discussions regarding the dissociation of I_2He complex.

APPENDIX A

In this section we indicate the procedure for obtaining Eq. (36). The v_y integrals from Eq. (29) of the first first terms in Eqs. (34) and (35) are of the form

$$\int_0^\infty dv_y\, v_y (e^{-a(l_2/v_y)} - e^{-a(l_1/v_y)}) e^{-v_y^2 c_0} \tag{A1}$$

with

$$a = \tfrac{1}{2}(\mu \cdot \mathcal{E}/\hbar)^2 (1/2T_1)\Lambda^{-1} . \tag{A2}$$

One would like to expand the exponentials to perform the integrations. However, with this scheme there would be inaccuracies at the lower limit of the integration. These problems may be eliminated to good approximation by stipulating that $|al_2|$, $|al_1| \ll 1/\sqrt{c_0}$ and $\mu \cdot \mathcal{E}/\hbar \ll 1/2T_1$. With this approximation

$$\int_0^\infty dv_y a(l_1 - l_2) e^{-v_y^2 c_0} = -\frac{1}{2}\sqrt{\pi/c_0}\, aL . \tag{A3}$$

The v_y integrals of the second terms cannot be performed in a similar fashion as the expansions are not valid. This is not alarming, however, since these integrals provide only multiplicative constants and do not determine the temporal decay characteristics that depend only on the Δ integration. Thus we define

$$I = \int_0^\infty dv_y\, v_y \exp(-v_y^2 c_0)(\exp(-l_2/v_y T_1) - \exp(-l_1/v_y T_1)) . \tag{A4}$$

Using these results in Eq. (29) gives

$$\bar{r}_2(t) = k_0 \bar{n}\, e^{-t/2T_1} \int_{-\infty}^{\infty} d\Delta\, e^{-\Delta^2 c_1} (f_2 \cos\Delta t - f_1 \sin\Delta t) ,$$

$$f_1 = \left[-\frac{1}{2}\sqrt{\frac{\pi}{c_0}} L\Delta\Lambda \left(\frac{\mu \cdot \mathcal{E}}{\hbar}\right) - \frac{1}{4} I\Delta T_1 \left(\frac{\mu \cdot \mathcal{E}}{\hbar}\right)^3 \right] \Lambda'^{-1} ,$$

$$f_2 = \left[-\frac{1}{2}\sqrt{\frac{\pi}{c_0}} L\Lambda \left(\frac{1}{2T_1}\right)\left(\frac{\mu \cdot \mathcal{E}}{\hbar}\right) + \frac{1}{8} I \left(\frac{\mu \cdot \mathcal{E}}{\hbar}\right)^3 \right] \Lambda'^{-1} ,$$

$$\Lambda' = \Lambda^2 - 2\left(\frac{\mu \cdot \mathcal{E}}{\hbar}\right)^2 \left(\frac{1}{2T_1}\right)^2 . \tag{A5}$$

For the case where the homogeneous linewidth of the transition is much smaller than the Doppler frequency width ($c_1 = 0$), the above integration can be done in a straightforward manner. The results in the low power regime give

$$\overline{r_2(t)} = A\, e^{-t/T_1} , \tag{A6}$$

where A is

$$A = k_0 \bar{n} \left(\frac{\pi}{2}\right) T_1^3 \left(\frac{\mu \cdot \mathcal{E}}{\hbar}\right)^3 \left[I - \frac{L}{T_1}\sqrt{\frac{\pi}{c_0}}\right]. \quad \text{(A7)}$$

The following comments can now be made: (a) Although this low power result of (A6) is similar in form to a bulb result, the physics of the decay processes is entirely different. Note that in Eq. (28) of the bulb the ground and the excited T_1 decay time constants are assumed to be the same. Using this equation and assuming that $T_2 = 2T_1$ will give different results. For the case where the ground and excited states T_1 are different the FID equation [see Eq. (4.24) of Ref. 38] is not valid for the beam case, where T_1 of the lower level goes to ∞, due to the fact that the steady state preparation is not done in a closed two level scheme[39]; and finally (b) In Eq. (A5), if c_1 is not equal to zero the integration can be done explicitly and yield conjugate error functions in addition to the usual decay terms. These error functions, however, modify the solution only at very short times. For the time scale of interest the exact solution agrees with the above Eq. (A6).

[1]S. A. Rice, in *Excited States*, edited by E. Lim, (Academic, New York, 1975), Vol. 2, p. 111.

[2]G. W. Robinson, in *Excited States*, edited by E. Lim, (Academic, New York, 1975), Vol. 1, p. 1.

[3]J. Jortner and S. Mukamel, in *The World of Quantum Chemistry*, edited by R. Dandel and B. Pullman, (Reidel, Dordrecht, 1974).

[4]K. F. Freed, Topics Appl. Phys. 15, 23 (1976).

[5]For a review, see R. Zare and P. Dagdigian, Science 185, 739 (1974).

[6]A. H. Zewail, T. E. Orlowski, and D. R. Dawson, Chem. Phys. Lett. 44, 379 (1976).

[7]A. H. Zewail, T. E. Orlowski, K. E. Jones, and D. Godar, Chem. Phys. Lett. 48, 256 (1977).

[8]A. H. Zewail, T. E. Orlowski, R. R. Shah, and K. E. Jones, Chem. Phys. Lett. 49, 520 (1977).

[9]T. E. Orlowski, K. E. Jones, and A. H. Zewail, Chem. Phys. Lett. 50, 45 (1977).

[10]N. F. Ramsey, *Molecular Beams* (Oxford U. P., London, 1956); P. Kusch and V. W. Hughes, in *Handbuch der Physik* (Springer, Berlin, 1959), Vol. 37, Part 1; T. C. English and J. C. Zorn, in *Methods of Experimental Physics* (Academic, New York, 1974), Vol. 3, p. 669.

[11]D. R. Herschbach, Adv. Chem. Phys. 10, 135 (1966); R. A. Larsen, S. K. Noeh, and D. R. Herschbach, Rev. Sci. Instrum. 45, 1511 (1974).

[12]J. B. Anderson, R. P. Andres, and J. B. Fenn, Adv. Chem. Phys. 10, 275 (1966).

[13]J. M. Farrar and Y. T. Lee, Ann. Rev. Phys. Chem. 25, 357 (1974).

[14]T. R. Dyke, G. R. Tomasevich, W. Klemperer, and W. E. Falconer, J. Chem. Phys. 57, 2277 (1972).

[15]T. J. Ryan, D. G. Youmans, L. A. Hackel, and S. Ezekiel, Appl. Phys. Lett. 21, 320 (1972); S. Ezekiel and R. Weiss, Phys. Rev. Lett. 20, 91 (1968).

[16]R. E. Smalley, B. L. Ramakrishna, D. H. Levy, and L. Wharton, J. Chem. Phys. 61, 4363 (1974).

[17]F. Bloch, Phys. Rev. 70, 460 (1946); see also L. Allen and J. H. Eberly, *Optical Resonance and Two-Level Atoms* (Wiley Interscience, New York, 1975).

[18]L. Allen, B. Allen, and P. L. Knight, Opt. Commun. 20, 150 (1977).

[19]A. Icsevgi and W. E. Lamb, Jr., Phys. Rev. 185, 517 (1969).

[20]See, for example, U. Fano, Rev. Mod. Phys. 29, 74 (1957); D. ter Haar, Rep. Prog. Phys. 24, 304 (1961); R. McWeeny, Rev. Mod. Phys. 32, 335 (1960).

[21]R. P. Feynman, F. L. Vernon, Jr., and R. W. Hellworth, J. Appl. Phys. 28, 49 (1957).

[22]A. Abragam, *The Principles of Nuclear Magnetism* (Oxford U. P., London, 1961).

[23]I. I. Rabi, N. F. Ramsey, and J. Schwinger, Rev. Mod. Phys. 26, 167 (1954).

[24]M. Sargent III, M. Scully, and W. Lamb, Jr., *Laser Physics* (Addison-Wesley, New York, 1974).

[25]See, for example, J. C. McGurk, T. G. Schmalz, and W. H. Flygare, in *Advances in Chemical Physics*, edited by I. Prigogine and S. A. Rice (Wiley, New York, 1974), Vol. XXV, p. 1; R. G. Brewer and R. L. Shoemaker, Phys. Rev. A, 6, 2001 (1972).

[26]F. A. Hopf, R. F. Shea, and M. O. Scully, Phys, Rev. A 7, 2105 (1973), and Ref. 25.

[27]For an excellent review, see R. Smalley, L. Wharton, and D. Levy, Acc. Chem. Res. 10, 139 (1977).

[28]P. Jacquinot, in *Topics in Applied Physics* (Springer, New York, 1976), Vol. 13.

[29]R. L. Shoemaker and E. W. van Stryland, J. Chem. Phys. 64, 1733 (1976).

[30]G. W. Series, in *Quantum Optics*, edited by S. M. Kay and A. Maitland (Academic, New York, 1970).

[31]The statistical distribution contains the usual Boltzmann factor but does not have any extraneous power of v as multiplicative factors. The flux through the slit is proportional to $v_y e^{-mv^2/2kT}$. However, in these experiments we are interested in the density. Thus we must divide the flux by the velocity through a plane perpendicular to the y axis (current). We therefore obtain the Maxwellian distribution without a v_y-dependent term in front of it. This point has been overlooked occasionally in the literature.

[32]J. L. Hall, in *Atomic Physics*, edited by S. Smith and G. Walters, (Plenum, New York, 1973), Vol. 3, p. 615; R. G. Brewer and G. Genack, Phys. Rev. Lett. **37**, 959 (1976).

[33]R. E. Smalley, D. H. Levy, and L. Wharton, J. Chem. Phys. **64**, 3266 (1976).

[34]W. Rhodes, J. Chem. Phys. **50**, 2885 (1969); J. Delory and C. Tric, Chem. Phys. **3**, 54 (1974); S. Mukamel and J. Jortner, in *Excited States* (Academic, New York, 1977), Vol. 3, in press; C. A. Langhoff and G. W. Robinson, Mol. Phys. **26**, 249 (1973); C. A. Langhoff, Chem. Phys. **20**, 357 (1977).

[35]J. Jortner and J. Kommandeur (to be published).

[36]See Ref. 35 and S. Mukamel and J. Jortner in Ref. 34; R. Lefebvre and J. Savolaimen, Chem. Phys. Lett. **3**, 449 (1969).

[37]J. P. Gordon, C. W. Wang, C. Patel, R. Slusher, and W. J. Tomlinson, Phys. Rev. **179**, 294 (1969).

[38]A. Schenzle and R. Brewer, Phys. Rev. A **14**, 1756 (1976).

[39]If *all* the emission is going back into the initial level, then the system is closed and the Bloch equations become somewhat different. If most of the emission is to levels other than the initial one, then the initial state will not be populated from other ground state levels since collisions are absent.